





RESEARCH ARTICLE

The therapeutic potential of an allosteric non-competitive CXCR1/2 antagonist for diabetic nephropathy

Chiara Grasselli¹ | Silvia Bombelli¹ | Vittoria D'Esposito² |
 Michele Francesco Di Tolla²  | Vincenzo L'Imperio^{1,3} | Francesca Rocchio⁴  |
 Martina Sara Miscione⁴ | Pietro Formisano² | Fabio Pagni^{1,3} | Rubina Novelli⁵ |
 Pier Adelchi Ruffini⁵  | Andrea Aramini⁶ | Marcello Allegretti⁶ |
 Roberto Perego¹  | Lidia De Filippis⁵

¹Department of Medicine and Surgery, University of Milano-Bicocca, Monza, Italy

²Department of Translational Medical Sciences, University of Naples Federico II, Naples, Italy

³Pathology Department, IRCCS Fondazione San Gerardo dei Tintori, Monza, Italy

⁴Dompé Farmaceutici S.p.A., Naples, Italy

⁵Research and Development, Dompé Farmaceutici S.p.A., Milano, Italy

⁶Dompé Farmaceutici S.p.A., L'Aquila, Italy

Correspondence

Lidia De Filippis.

Email: lidia.defilippis@dompe.com

Funding information

Ministero dello Sviluppo Economico; Ladarixin as new Juvenile Diabetes Inhibitory Agent; Fondo crescita sostenibile-Proposal, Grant/Award Numbers: DM 02/0872019, DD 02/10/2019

Abstract

Aims: Diabetic nephropathy is a major consequence of inflammation developing in type 1 diabetes, with interleukin-8 (IL-8)-CXCR1/2 axis playing a key role in kidney disease progression. In this study, we investigated the therapeutic potential of a CXCR1/2 non-competitive allosteric antagonist (Ladarixin) in preventing high glucose-mediated injury in human podocytes and epithelial cells differentiated from renal stem/progenitor cells (RSC) cultured as nephrospheres.

Materials and Methods: We used human RSCs cultured as nephrospheres through a sphere-forming functional assay to investigate hyperglycemia-mediated effects on IL-8 signalling in human podocytes and tubular epithelial cells.

Results: High glucose impairs RSC self-renewal, induces an increase in IL-8 transcript expression and protein secretion and induces DNA damage in RSC-differentiated podocytes, while exerting no effect on RSC-differentiated epithelial cells. Accordingly, the supernatant from epithelial cells or podocytes cultured in high glucose was able to differentially activate leucocyte-mediated secretion of pro-inflammatory cytokines, suggesting that the crosstalk between immune and non-immune cells may be involved in disease progression in vivo.

Conclusions: Treatment with Ladarixin during RSC differentiation prevented high glucose-mediated effects on podocytes and modulated either podocyte or epithelial cell-dependent leucocyte secretion of pro-inflammatory cytokines, suggesting CXCR1/2 antagonists as possible pharmacological approaches for the treatment of diabetic nephropathy.

KEYWORDS

CXCR1/2, diabetic nephropathy, IL-8, Ladarixin, renal stem cell, type 1 diabetes

Chiara Grasselli and Silvia Bombelli contributed equally to the study.

This is an open access article under the terms of the [Creative Commons Attribution-NonCommercial-NoDerivs](https://creativecommons.org/licenses/by-nc-nd/4.0/) License, which permits use and distribution in any medium, provided the original work is properly cited, the use is non-commercial and no modifications or adaptations are made.

© 2023 Dompé Farmaceutici S.p.A. and The Authors. *Diabetes/Metabolism Research and Reviews* published by John Wiley & Sons Ltd.

1 | INTRODUCTION

Diabetic nephropathy (DN) is the primary cause of renal failure in the western world and is associated with increased mortality in diabetic patients.¹ Although its biological drivers are still far from being fully characterised,² inflammation has been recognised as a key player in DN pathophysiology,^{2–4} and novel innovative strategies for targeting inflammation have been studied.^{5–7} Among all the factors involved in the DN-related inflammatory process, interleukin-8 (IL-8) has been suggested to be crucially involved in the onset and/or maintenance of DN.^{8–10}

IL-8 is a pro-inflammatory chemokine released by both immune and non-immune cells, including podocytes¹¹ and endothelium,¹² and acts as a chemotactic factor binding two membrane receptors, CXCR1 and CXCR2, which are both expressed by several cell types, including immune cells and podocytes.¹¹ Its levels have been found increased in the serum of both type 1 and type 2 diabetes patients¹³ and associated to insulin resistance and metabolic disease.¹³ Supporting its role in DN, previous studies have shown that IL-8 levels are elevated in the urine of patients with type 2 diabetes and strongly associated with a reduced renal function and worse clinical outcome.¹⁴ Interestingly, IL-8 release is strongly enhanced during high glucose challenge of podocytes *in vitro*, suggesting that hyperglycemia may trigger podocyte IL-8 production in type 2 diabetes patients, thus activating death signals in CXCR1/CXCR2-expressing podocytes through an autocrine loop and favouring DN.^{12,14} However, the mechanisms underpinning IL-8 action in DN and its biological targets, as well as the potential therapeutic significance of its pharmacological blockade, have never been fully investigated.

One of the main limiting factors when studying pathways and potential targets involved in DN is the lack of adequate human models able to reproduce the three main cell lineages of the kidney (tubules, podocytes and endothelium). To meet this need, a new model has been recently developed¹⁵ using human renal stem/progenitor cells (RSCs) cultured as nephrospheres (NS) through the sphere-forming functional assay.^{16,17} Within the NS, cells have different levels of maturation, with a homogeneous cell population displaying *in vitro* self-renewal and the capacity to differentiate into tubular epithelial cells, podocytes and endothelial cells.¹⁵ Notably, NS cells have displayed the capability to fully differentiate into podocytes expressing several podocyte-specific markers such as synaptopodin, nestin, and alpha-actinin markers in addition to podocin.¹⁵ NS is thus a physiological model that allows faithfully resembling the features of human primary cells and, simultaneously, study systems deriving from different patients. These features make the NS an optimal model to study the mechanisms that regulate self-renewal and differentiation in adult renal tissue as well as in renal pathological conditions, such as DN, and to test new drugs.

In this study, we used the NS model to investigate hyperglycemia-mediated effects on IL-8 signalling in human podocytes and tubular epithelial cells and to evaluate the potential effects of the

pharmacological blockade of the IL-8-CXCR1/2 axis in preventing IL-8-mediated damage and, eventually, in modulating the onset and progression of DN.

2 | MATERIALS AND METHODS

2.1 | Tissues

Normal kidney tissue was obtained from 8 patients following nephrectomy due to the presence of renal tumours. The normal tissue was taken from a healthy region of the kidney, without any indication of cancer, opposite to the tumour and exceeding the diagnostic needs. All procedures were performed after written patient consent and approved by the Local Ethical Committee. NS cultures were established from all fresh renal tissue samples.

2.2 | Nephrosphere cultures, epithelial and podocyte differentiation, rIL-8 and Ladarixin treatment

The single-cell suspension from the renal tissue and the NS cultures were obtained from 8 different tissue samples and cultured as NS as described.¹⁵

The suspension obtained after mechanical dissociation and enzymatic digestion was sieved through a 250 µm cell strainer and then passed through a pipette syringe to obtain a single-cell suspension. Red blood cells were removed by haemolysis with 0.8% NH₄Cl solution for 5 min. After a 24–48 hours adhesion step, the trypsinised bulk epithelial cells were plated (10,000 cells/mL) in Stem Cell medium in physiological (17 mM) and high glucose conditions (30 mM) on poly-Hema (Sigma Aldrich, St. Louis, MO) coated dishes in non-adherent conditions for the formation of floating NSs. After 10 days, NS were collected for use.

For the evaluation of SFE, the number of obtained spheres was divided by the number of plated renal cells and expressed as a percentage.

For cell differentiation or FACS analysis, after 10 days NS were collected for use. NS cells were dissociated enzymatically for 5 min in TrypLE Express (Life Technologies, Waltham, MA) and then mechanically by repetitive pipette syringing to generate a single-cell suspension.

Single cells obtained from nephrospheres were then subjected to epithelial and podocyte differentiation for 7 days in physiological (17 mM) and high glucose conditions (30 mM) in specific differentiation media. The specific differentiation media were as follows: epithelial medium, composed of Dulbecco's modified Eagle's medium-F12 (Lonza, Basel, Switzerland) supplemented with 10% foetal bovine serum, ITS supplement (5 µg/mL insulin, 5 µg/mL transferrin, and 5 ng/mL sodium selenite), 36 ng/mL hydrocortisone, and 40 pg/mL triiodothyronine (all from Sigma-Aldrich), 20 ng/mL epithelial growth factor (Cell Signalling Technology), and 50 ng/mL hepatocyte growth

factor (Cell Signalling Technology); VRADD podocyte medium, composed of Dulbecco's modified Eagle's medium-F12 (Lonza, Basel, Switzerland) supplemented with 10% foetal bovine serum, 100 nM D3 Vitamin, 100 μ M Retinoic Acid, 0.1 μ M Dexamethasone. Recombinant IL-8 protein (rIL-8, ChinaPeptides, Shanghai, China) treatment was performed by adding rIL-8 100 ng/mL rIL-8 to the culturing media. CXCR1/2 blockade was achieved by culturing the cells in a medium containing Ladarixin 1 μ M or 10 μ M.

2.3 | Immunofluorescence and FACS analysis

IF on differentiated cells grown on coverslips was performed as described¹⁵ using the mouse monoclonal anti-CXCR1 (clone 501, Invitrogen, 1:100), mouse monoclonal anti-CXCR2 (clone GT547, Invitrogen, 1:100), mouse monoclonal anti-pan Cytokeratin (clone MNF116, DAKO; 1:200), rabbit anti-Podocin (Sigma Aldrich, 1:50) primary antibodies and Alexa Fluor 488 conjugated anti-mouse and Alexa Fluor 594 conjugated anti-rabbit IgG secondary antibodies (Molecular Probes Invitrogen, 1:100). IF micrographs were obtained at 400x magnification using a Zeiss LSM710 confocal microscope and Zen2009 software (Zeiss). For DNA damage analysis, mouse monoclonal anti-phospho- Histone H2A.X (Ser 139) (clone JBW301, Millipore; 1:100) primary antibody was used. Percentages of labelled cells over the total nuclei and the number of foci per nucleus were evaluated. The number of foci per nucleus was determined using-Count Nuclear Foci Plugin-ImageJ software version 1.53c (National Institute of Health, NIH; <http://imagej.nih.gov/ij>).

The FACS procedure was performed on NS preparations and differentiated cells, and analysis was performed using a MoFlo Astrios Cell Sorter equipped with Summit software version 6.1 (Beckman Coulter, Milano, Italy). The offline analysis was performed using Kaluza software version 1.2 (Beckman Coulter, Brae, CA). For FACS analysis, the following antibodies were used: mouse monoclonal FITC-conjugated anti-CXCR1 (clone 8F1, Miltenyi Biotec; 1:10) and mouse monoclonal APC Vio770-conjugated anti-CXCR2 (clone REA208, Miltenyi Biotec; 1:50).

Cell viability of dissociated nephrospheres and differentiated cells was evaluated using the APC Annexin V Apoptosis detection kit and propidium iodide (Biolegend, San Diego, CA), according to the manufacturer's instructions, as previously described.¹⁸ FACS analysis was performed on 10,000 events with a MoFlo Astrios Cell Sorter equipped with Summit software version 6.1 (Beckman Coulter, Milano, Italy). The offline analysis was performed using Kaluza software version 1.2 (Beckman Coulter, Brae, CA). Viable cells (annexin V and propidium iodide negative) were expressed as a percentage with respect to the total events analysed.

2.4 | Western blot

Cell lysates were prepared, separated by SDS Nupage 4%–12% and blotted on a nitrocellulose membrane (all Life Technologies) as

described.¹⁹ The protein standard Dual Colour Marker loaded on the gel was from Bio-Rad. The blotted membranes were probed with antibodies against CXCR1 (clone 501, Invitrogen, 1:1000), mouse monoclonal anti-CXCR2 (clone GT547, Invitrogen, 1:1000). ECL (Pierce, Thermo Fisher Scientific) detected the antigen-antibody complexes. The densitometry of the bands was analysed by ImageJ software (NIH).

2.5 | Real time PCR

Total RNA extracted from differentiated cells was reverse transcribed with the high-capacity cDNA Reverse Transcription Kit (Applied Biosystems, Waltham, MA). TaqMan gene expression real-time PCR assays were performed in duplicate for each sample, following manufacturer's instructions using the indicated commercial kits (IL8: Hs00174103_m1; GAPDH: Hs99999905_m1) and an ABI PRISM 7900HT Fast Real-Time PCR System (Applied Biosystems). The expression fold change between the different cell treatments was calculated as $2^{-\Delta\Delta Ct}$ always using cells cultured in physiological glucose conditions as a calibrator.

2.6 | Secreted IL-8 quantification by ELISA

IL-8 in cell culture medium was quantified with a Human IL-8 ELISA kit (Sigma Aldrich, St. Louis, MO) according to the manufacturer's instructions and using a microplate reader (Victor Wolla C1420, Perkin Elmer, Waltham, MA). Concentration values (pg/mL) were normalised to concentrate protein extracted from each sample and then represented as a ratio between high glucose (HG) and physiological conditions (NG).

2.7 | Cytokines, chemokines and growth factors quantification by ELISA multiplex assay

Supernatants from podocytes, epithelial cells, and from leucocytes incubated these supernatants, were screened for the concentration of IL-1 β , IL-1ra, IL-2, IL-4, IL-5, IL-6, IL-7, IL-8, IL-9, IL-10, IL-12 (p70), IL-13, IL-15, IL-17A, basic fibroblast growth factor (FGF), eotaxin, granulocyte-colony stimulating factor (G-CSF), granulocyte-macrophage colony-stimulating factor (GM-CSF), interferon- γ (IFN- γ), interferon- γ inducible protein 10 (IP-10), monocyte chemoattractant protein-1 (MCP-1), macrophage inflammatory protein-1 (MIP-1) α , MIP-1 β , C-C motif chemokine ligand 5 (CCL5)/RANTES, tumour necrosis factor- α (TNF- α), platelet-derived growth factor (PDGF-BB), and vascular endothelial growth factor (VEGF) using the Bio-Plex Multiplex Human Cytokine, Chemokine, and Growth Factor Kit (cat. n. M500KCAF0Y, Bio-Rad, Hercules, CA, USA) according to the manufacturer's protocol, as previously described.²⁰ The magnetic bead-based assay was performed on a Bio-Plex 200 System (Bio-Rad, Hercules, CA, USA).

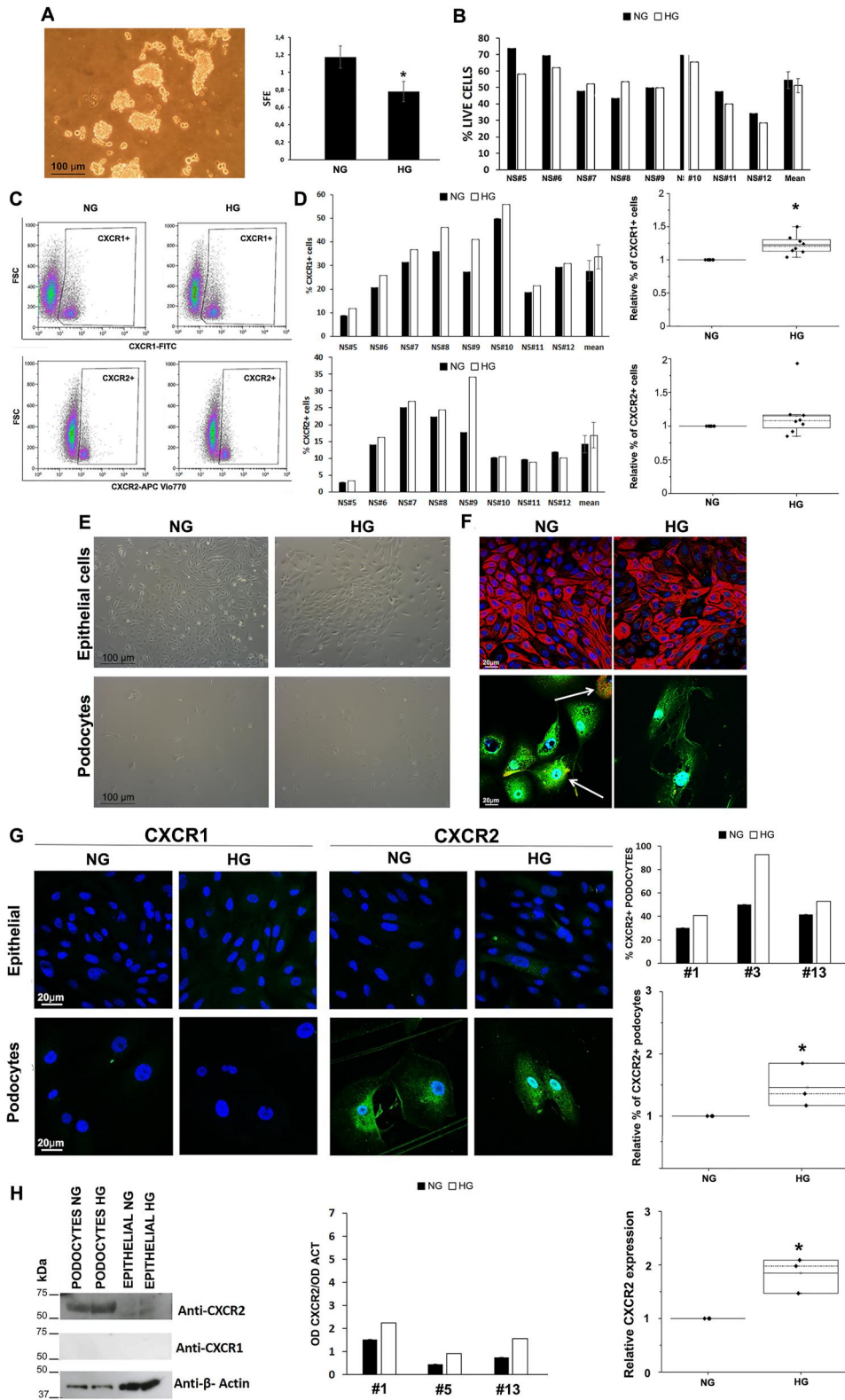


FIGURE 1 Legend on next page.

2.8 | Pathology and immunohistochemistry

Consecutive formalin-fixed paraffin-embedded (FFPE) renal samples were retrospectively retrieved from the archives of the Pathology

Department of ASST Monza (San Gerardo Hospital), UNIMIB, Italy. In particular, specimens corresponding to the renal parenchyma distant from the neoplasia in nephrectomies for renal cancer were selected avoiding cases affected by diabetic nephropathy (DN). In a similar

way, renal biopsies with a diagnosis of DN without concurrent other kidney diseases were retrospectively enrolled from the Nephropathological archives. These cases have been reviewed by two expert renal pathologists (VL and FP) and classified according to the Tervaert scheme as 'early' (class I-II), 'moderate' (class III) and 'advanced DN' (class IV).²¹ Baseline clinical characteristics (age, sex, hypertension, serum creatinine and proteinuria) were recorded for each case. For immunohistochemistry (IHC), 3 μ m FFPE sections from the cases were deparaffinised and rehydrated. After endogenous peroxidase blockage and antigen retrieval with EnVision FLEX Target Retrieval Solution (Dako, Glostrup, Denmark), the slides were incubated with the primary antibody in the Dako Omnis stainer. Multiple washes were performed, and then the secondary antibody conjugated with peroxidase was applied. Finally, the specimens were washed in PBS and developed in 3,3'-diaminobenzidine (DAB) for single IHC for CD3 and in DAB and aminoethyl carbazole (AEC) for double IHC directed to nuclear γ -H2AX and membrane phospholipase A2 receptor (PLA2R) and cytokeratin 8/18 (CK 8/18), as previously.^{22,23} The following primary antibodies were used: polyclonal rabbit anti-human CD3 (prediluted, ready-to-use, Dako), monoclonal mouse anti- γ -H2AX (anti-phospho-histone H2AX, Ser139, clone JBW301, dilution 1:500; Millipore, Billerica, MA, USA), rabbit polyclonal antibodies against PLA2R (Atlas Antibodies, AlbaNova University Center, Stockholm, Sweden, concentration 0.4 mg/mL, dilution 1:300), monoclonal anti-human CK 8/18 (prediluted, ready-to-use, Dako).

2.9 | Digital and computational pathology

Slides from both histochemistry (periodic acid of Schiff, PAS) and IHC for all the cases were scanned using the newly introduced hybrid MIDI II instrument (3DHISTECH, Budapest, Hungary).²⁴ The obtained whole slide images (WSI) in .mrxs format have been imported in the QuPath v0.3.2 software for the computational analysis.²⁵ Normal and globally sclerosed glomeruli have been comprehensively annotated. The total number of cells in the whole biopsy and in the glomerular region was calculated through the 'Cell detection' function. For the detection of inflammatory cells in the biopsy, a cell

classifier was trained and applied to all cases to quantify the number of infiltrates. Cells positive for IHC were quantified using alternatively the 'Positive cell detection' and 'Cell intensity classification' functions.

2.10 | Statistical analysis

Dichotomous variables were compared using the chi-square test. Continuous variables are expressed as mean \pm standard deviation (SD) or as mean (95% CI). All groups were compared for clinical and histological continuous variables using the one-way ANOVA test for independent variables. All *p*-values were two-tailed and values <0.05 were considered statistically significant.

Statistical analysis was performed using the software Excel (Microsoft, Redmond, Washington, USA) and SPSS Statistics (v26.0. Armonk, NY: IBM Corp.) and the GraphPad Prism 8.0 software (GraphPad Software Inc., La Jolla, Ca).

3 | RESULTS

3.1 | High glucose inhibits RSC self-renewal

To investigate the effects of high glucose on NS, we cultured NS obtained from human renal tissue samples ($n = 8$; Figure 1A) under physiological (NG) (17 mM) or high glucose (HG) conditions (30 mM), thus mimicking a diabetic-like environment. First, we assessed the sphere forming efficiency (SFE) as a measure of self-renewal capability of NS cells. A decrease in SFE was observed in all NS cultured under HG compared with those cultured under NG (Figure 1A). To verify whether this result was due to an effect of glucose on cell viability, we evaluated the viability of NS cells exposed to HG by Annexin V/PI FACS assay. Notably, no significant changes were observed compared to NG (Figure 1B), suggesting that the lower SFE of RSCs in HG was not related to increased cell death but to a HG-mediated effect on self-renewal potential.

We then investigated whether the IL-8/CXCR1-2 axis could be involved in the effects of HG on NS cells. Thus, we first analysed the

FIGURE 1 (A) Representative contrast phase image of nephrospheres (10x magnification); scale bars: 100 μ m (left) and Mean \pm SEM sphere forming efficiency (SFE) representation in eight different NS samples (right). (B) Percentage of live cells in eight different NS cultures and the mean \pm SEM percentage in the eight samples. (C) Representative FACS analysis of CXCR1 and CXCR2 expression on nephrosphere cells cultured in high glucose and physiological conditions. (D) Histogram representing the CXCR1+ and CXCR2+ cell percentage (left) and scatter plot of CXCR1+ and CXCR2+ cell percentage represented as fold change (right) ($n = 8$). NG: physiological conditions. HG: high glucose conditions. (E) Representative contrast phase images of epithelial and podocyte differentiated cells (10x magnification); scale bars: 100 μ m. (F) Representative immunofluorescence analysis using antibodies against pan cytokeratin (red) and podocin (green) on NS cells differentiated into epithelial cells and podocytes (40x magnification) in physiological (NG) and high glucose (HG) conditions. Blue: DAPI. White arrows indicate cells expressing both Cytokeratin and Podocin. Scale bars: 20 μ m. (G) Representative immunofluorescence analysis using antibodies against CXCR1 and CXCR2 on NS cells differentiated into epithelial cells and podocytes (40x magnification) in physiological (NG) and high glucose (HG) conditions. Scale bars: 20 μ m (left). Graphical representation of CXCR2+ cell count in three different podocyte cultures and scatter plot of CXCR2+ cells represented as fold change (right). (H) Representative Western Blot analysis of CXCR1 and CXCR2 expression of culture #1 (left) and CXCR2 densitometry of three analysed podocyte cultures and scatter plot of relative CXCR2 protein expression represented as fold change (right). **p* < 0.05.

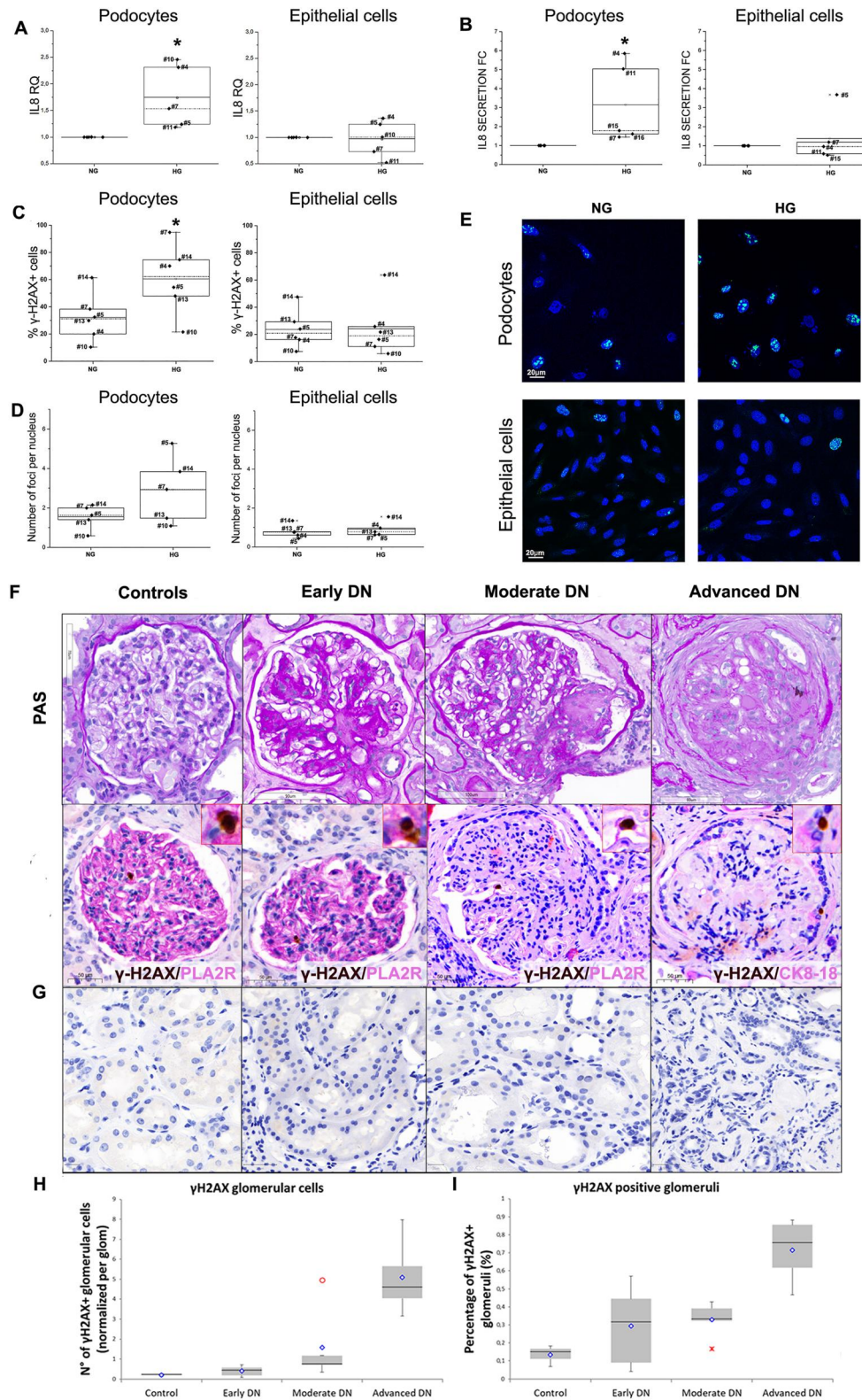


FIGURE 2 Legend on next page.

expression of IL-8 receptors, CXCR1 and CXCR2, in NS cells under NG and HG. FACS analysis of immature NS cells cultured in HG showed that the percentage of CXCR1+ was higher in all the tested

NS cultures, while that of CXCR2+ cells was increased ($n = 6/8$) in HG NS cultures compared to those in NG (Figure 1C–D). Due to the high individual variability of the human biological samples, we

expressed the data as fold change of CXCR1+ and CXCR2+ NS cells under HG versus NG. Notably, CXCR1+ cells were significantly more abundant in NS cultured in HG (Figure 1D).

After 7 days of NS ($n = 6$) differentiation under NG or HG, contrast phase microscopy morphology and immunofluorescence analyses showed that we obtained epithelial and podocyte differentiated cells (Figure 1E).

Epithelial-differentiated cells expressed pan cytokeratin (red), whereas no podocin staining was observed; on the other hand, podocyte-differentiated cells were positive for podocin (green) and showed a fainting cytokeratin staining (Figure 1F). Notably, we could still observe some podocyte-differentiated cells co-expressing cytokeratin and podocin (Figure 1F, arrows), likely indicating different differentiation timings.

Contrary to what was observed in immature NS cells (Figure 1C–D), immunofluorescence (Figure 1G) and western blot (Figure 1H) analyses showed that terminally differentiated podocytes and epithelial cells did not express CXCR1 in both NG and HG. CXCR2 expression was evident in both cell types and was much higher in podocytes than in epithelial differentiated cells. While epithelial cells showed no differences, the percentage of CXCR2+ cells was significantly higher in podocyte cultures grown in HG versus NG (Figure 1G–H). These observations suggest that a diabetic-like environment may physiologically enhance the activation of the CXCR2 receptor in terminally differentiated podocytes.

3.2 | Effect of high glucose in human podocytes

To assess if the HG-induced increase in CXCR2 expression in podocytes would be associated with an increment in the expression of the ligand IL-8, we evaluated IL-8 expression in cultures differentiated under NG or HG. HG induced an evident increase in IL-8 expression at transcript level in all podocyte- but not in epithelial differentiated cells (Figure 2A). In line with RT-PCR data, ELISA results also showed

that IL-8 secretion was significantly increased in the culture media of podocyte-differentiated cells (Figure 2B).

Then, starting from previous studies that linked DN with DNA damage,^{14,26–28} we evaluated DNA damage by γ -H2AX immunofluorescence on podocyte and epithelial differentiated NS cells. The percentage of γ -H2AX+ cells (Figure 2C) was significantly increased in podocytes cultured in HG compared to NG, while the number of foci per nucleus was still higher in HG compared to NG in all the podocyte cultures tested but did not show statistical significance due to the high variability among the samples (Figure 2D). On the contrary, HG did not affect DNA damage in epithelial cells (Figure 2C–D), thus suggesting that podocyte DNA damage was glucose-dependent and cell type-specific.

3.3 | DNA damage increases with the progression of DKD

To investigate whether the DNA damage can be a key factor in the progression of Diabetic Kidney Disease (DKD) in patients, IHC directed against γ -H2AX was performed also on biopsy sections from controls ($n = 3$), early ($n = 5$), moderate ($n = 5$) and advanced DKD patients ($n = 4$), whose clinical and histological details are reported in Table 1.

Histological analysis of cases with progressively more severe DKD (from controls to advanced cases) demonstrated a worsening of the collagen deposition in the mesangial areas, causing progressive sclerosis (from diffuse, to nodular and global glomerulosclerosis), as highlighted by PAS stain (Figure 2F). The analysed cases did not show any difference in terms of clinico-pathological features apart from a progressive higher serum creatinine (mg/dL), proteinuria (g/day) and percentage of globally sclerosed glomeruli towards advanced DKD (Table 1). Nuclear γ -H2AX positivity was found in glomeruli from all the analysed patients within podocytes (as demonstrated by the double positivity for γ -H2AX in brown and PLA2R in pink) and,

FIGURE 2 (A) Scatter plot of real-time PCR analysis of IL-8 transcript in the indicated culture conditions. RQ: Relative quantification expressed as $2^{-\Delta\Delta Ct}$ of five different podocytes and epithelial cultures. Podocyte and epithelial cells cultured under physiological conditions (NG) were used as calibrators. * $p < 0.05$. (B) Scatter plot of IL-8 secretion measured in 5 podocyte and epithelial cultures by ELISA. Data have been normalised to the concentration of protein extracted from each sample and then represented as a ratio between high glucose (HG) and physiological conditions (NG). Continuous line: mean. Dotted line: median. * $p < 0.05$. (C) Scatter plot of γ -H2AX+ cell percentage in six different podocytes and epithelial cultures. * $p < 0.05$. (D) Scatter plot of the mean number of γ -H2AX foci per nucleus evaluated in five different podocytes and epithelial cultures. Continuous line: mean. Dotted line: median. (E) Representative immunofluorescence analysis using antibodies against γ -H2AX on NS cells differentiated into podocytes and epithelial cells in physiological (NG) and high glucose (HG) conditions (40x magnification); scale bars: 20 μ m. In (F), the spectrum of histological aspects of cases analysed with increasing glomerular sclerosis from the 'control' to the advanced DN cases, as demonstrated by the PAS stain. Specifically, healthy controls did not show a significant increase in mesangial collagen matrix, which becomes more evident in early DN (so-called diffuse glomerulosclerosis), with initial formation of sclerotic nodules in moderate DN (nodular glomerulosclerosis), to the complete obliteration of the glomerular tuft in advanced DN (global glomerulosclerosis), the first row. In the second row, the nuclear positivity for the γ -H2AX IHC (brown, DAB) is restricted to the podocytes, as demonstrated in the upper right insets using the double positivity with membrane PLA2R (pink, AEC). In advanced DN, scattered positive cells in globally sclerosed glomeruli showed double nuclear (for γ -H2AX in brown) and membrane (for CK8/18 in pink) positivity, as shown in the upper right inset, demonstrating their parietal epithelial origin. As compared to the positivity recorded in glomeruli, tubules did not show any positivity in all the cases tested from controls to advanced DN, as shown in the third row (G). The distribution of absolute γ -H2AX+ cells in glomeruli (H) as well as the percentage of glomeruli with at least one γ -H2AX+ cell (I) demonstrated a trend towards increased DNA damage with the progression of DN (p -value of 0.01 and 0.03, respectively).

TABLE 1 Clinical and histological characteristics of the cases.

Case #	Age (y)	Sex	Hypertension (±)	N° glomeruli	Globally sclerosed glomeruli	Serum creatinine (mg/dL)	Proteinuria (g/die)
CTR1	63	M	+	290	0	1,1	0,1
CTR2	69	M	+	198	0	1,2	0,2
CTR3	63	F	–	256	0	1	0,1
Early DN1	71	M	+	7	2	1	2,3
Early DN2	71	M	+	9	1	2,2	3
Early DN3	62	M	+	11	1	0,8	5
Early DN4	56	M	+	19	4	0,9	1
Early DN5	38	F	+	24	2	2,4	7
Moderate DN 1	60	M	+	34	1	1,4	8,3
Moderate DN 2	47	M	+	24	11	1,3	4
Moderate DN 3	52	M	–	35	12	3,4	6,4
Moderate DN 4	35	F	+	23	11	1,2	3,5
Moderate DN 5	71	M	+	27	13	5,9	2,7
Advanced DN 1	32	F	–	6	3	3,2	6
Advanced DN 2	43	F	+	39	27	5,29	5
Advanced DN 3	44	M	+	15	15	7	4,24
Advanced DN 4	50	M	+	17	1	2,5	7

occasionally, in parietal epithelial cells (as demonstrated by the double positivity for γ -H2AX in brown and CK 8/18 in pink), especially in globally sclerosed glomeruli of advanced DKD cases (Figure 2F), while no staining was noted in tubular cells of patients at all DKD stages (Figure 2G). The distribution of absolute γ -H2AX + glomerular cells normalised for the number of glomeruli indicated a progressive increase in DNA damage from controls to advanced DKD (Figure 2H). A similar trend was also observed by comparing the percentage of glomeruli with at least one γ -H2AX+ positive glomerular cell, suggesting a progressively widening involvement of multiple glomeruli in the DNA damage through DKD progression (Figure 2I).

3.4 | Exogenous IL-8 mimics but does not enhance high glucose-induced damage

Previous studies showed that both HG and exogenous IL-8 were needed to induce a remarkable DNA damage in human immortalised podocytes.¹⁴ Thus, having demonstrated that HG can induce DNA damage in NS-derived podocytes, we then tested whether supplementation with exogenous IL-8 could further increase DNA damage.

After differentiation under NG and HG in the presence or absence of 100 ng/mL IL-8 for 7 days, DNA damage was assessed by γ -H2AX immunofluorescence analysis. The percentage of γ -H2AX + cells (Figure S1A), as well as the number of foci per nucleus (Figure S1B), progressively increased in podocytes cultured in NG with IL-8

and in HG compared to NG, while no effect was observed in epithelial cells under the same conditions (Figure S1C,D). Notably, the addition of IL-8 did not exacerbate the HG-induced podocyte DNA damage, as the percentage of γ -H2AX+ cells was similar to that observed under NG with IL-8 (Figure S1A–D). A variable but similar trend was observed for IL-8 gene expression (Figure S1E–F).

These results suggest that exogenous IL-8 does not exacerbate autologous IL-8 expression activation as well as the DNA damage in human NS-derived podocytes cultured in a diabetic-like environment.

3.5 | Effect of Ladarixin on human podocytes

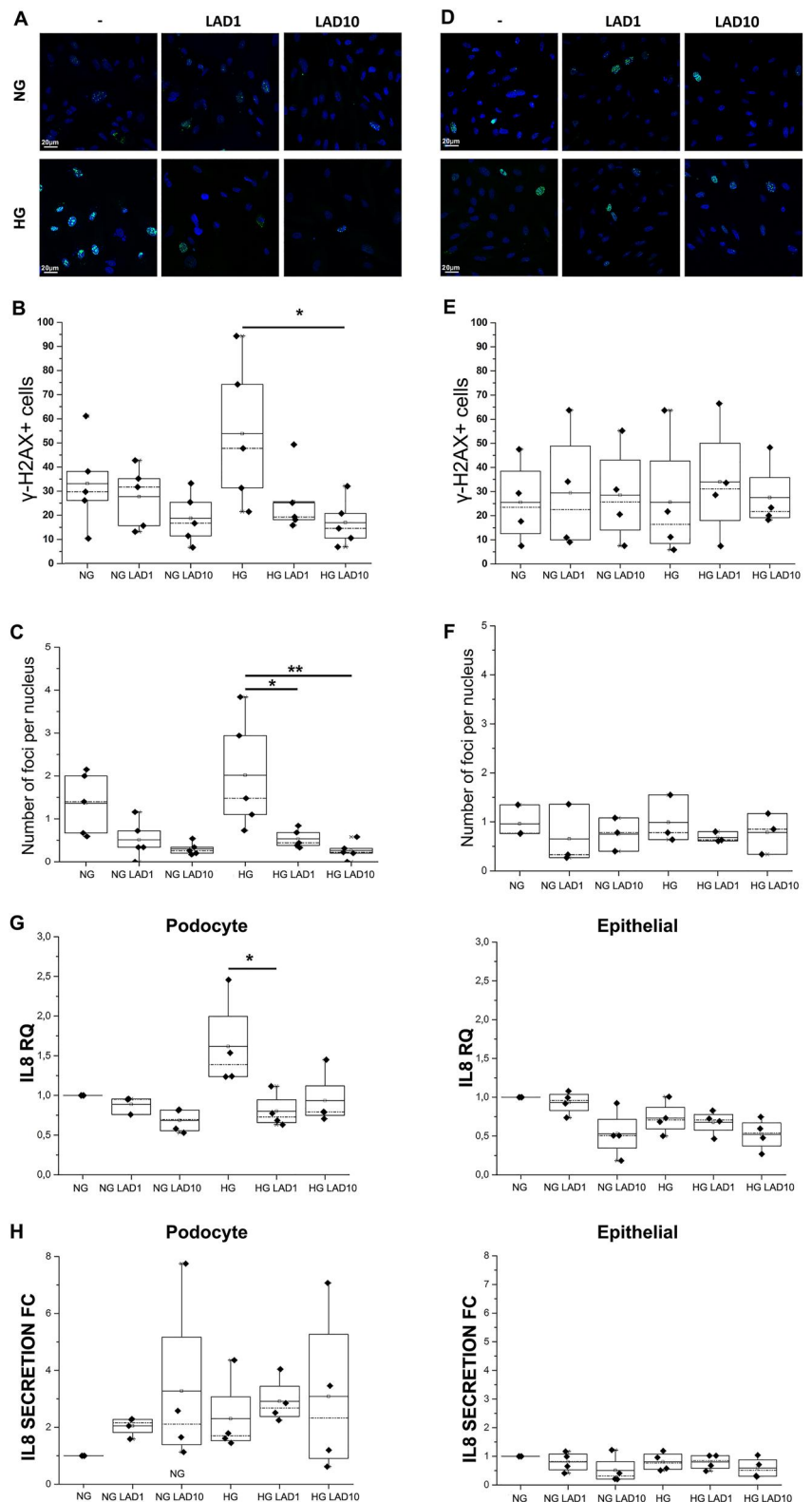
With the perspective to prevent the podocyte damage induced by spontaneous IL-8 production by podocytes cultured in HG, we antagonised IL-8 pathway using a specific non-competitive allosteric inhibitor of CXCR1/2 (Ladarixin).^{29–32}

We cultured podocytes and epithelial cells from the differentiation of NS under NG and HG in presence or absence of 1 μ M (LAD1) or 10 μ M Ladarixin (LAD10) for 7 days.

AnnexinV/PI FACS analysis showed that HG as well as drug treatment did not affect cell viability of podocyte and epithelial cultures (Figure S2A–B), showing that Ladarixin is well-tolerated by human NS-differentiated cells.

We then evaluated DNA damage by γ -H2AX immunostaining on podocyte and epithelial cultures. As the percentage of γ -H2AX + podocytes increased in HG (Figure 3A), Ladarixin at both tested

FIGURE 3 Representative immunofluorescence analysis using antibodies against γ -H2AX on NS cells differentiated into podocytes (panel (A), (B), (C)) and epithelial cells (panel (D), (E), (F)) in physiological (NG) and high glucose (HG) conditions with or without Ladarixin treatment (40x magnification); scale bars: 20 μ m. Scatter plot of γ -H2AX+ cell percentage in five different podocyte (B) and four epithelial (E) cultures. Continuous line: mean. Dotted line: median. Scatter plot representing the number of γ -H2AX foci per nucleus evaluated in four different podocyte (C) and three epithelial (F) cultures. * $p < 0.05$. ** $p < 0.01$. LAD1: 1 μ M Ladarixin. LAD10: 10 μ M Ladarixin. Scatter plot of real-time PCR analysis of IL8 transcript in the indicated culture conditions. (G) RQ: Relative quantification expressed as $2^{-\Delta\Delta Ct}$ of four different podocytes (left) and epithelial (right) cultures. Continuous line: mean. Dotted line: median. * $p < 0.05$. (H) Scatter plot of IL-8 secretion measured by ELISA in four podocyte (left) and epithelial (right) cell cultures. Values were normalised over total protein amount.



concentrations almost completely prevented DNA damage (Figure 3A–B), reaching a significant effect at 10 μ M. A similar effect was observed on the number of foci per nucleus (Figure 3C). Neither HG nor Ladarixin treatment affected DNA damage in epithelial differentiated cells (Figure 3D–F).

To assess whether the inhibition of CXCR1/2 by Ladarixin also resulted in a reduction of IL-8 gene expression, we evaluated the expression of IL-8 transcript and IL-8 secretion in the differentiated cells treated with Ladarixin. IL-8 transcript expression in podocyte-differentiated cultures increased under HG compared to

NG and the presence of Ladarixin counteracted this increment (Figure 3G). ELISA confirmed the increment of IL-8 secretion after HG treatment in podocyte-differentiated cultures, while in this case Ladarixin did not affect this increment (Figure 3H). In epithelial cells, the different concentrations of glucose and Ladarixin did not influence both IL-8 expression (Figure 3G) and secretion (Figure 3H).

These results suggest that HG-mediated induction of IL-8 pathway in podocytes is self-sustained through the activation of autologous IL-8 production, and Ladarixin-mediated inhibition of IL-8 pathway can thus be a possible therapeutic solution.

3.6 | CD3+ T lymphocytes increase during the progression of DN

Since the presence of inflammatory infiltrates of activated immune cells is well documented in the glomeruli affected by DN,^{33,34} we hypothesised that IL-8 produced by podocytes may induce the recruitment of immune cells from the circulation and the stimulation of the resident immune cells.

To investigate whether the interstitial inflammatory infiltrates are modified in intensity and composition during the DN progression, whole and CD3+ interstitial inflammatory infiltrates were quantified in renal biopsies of DN patients at different stages. Analysis of the whole inflammatory interstitial infiltrate did not show statistically significant differences for the number and the area covered by the interstitial inflammatory cells, either in absolute terms or as a ratio of the whole cellular component of the biopsy, among groups. On the other hand, when the CD3+ infiltrates were quantified, a statistically significant increase was noted in terms of T-cell/total inflammatory cell count (Figure 4A) and area ratios among groups (Figure 4B), as

also shown by histology analysis and digital pathology output (Figure 4C).

IL-8 secreted by non-immune cells is known to play a key role in the chemotactic migration of leucocytes to the lesioned area. We hypothesised that IL-8 secreted by podocytes under HG conditions may attract and stimulate leucocytes as a self-defence mechanism at the early stage of the disease development, thus becoming detrimental with inflammatory progression. To validate this hypothesis, we performed a cytokine screening by Luminex of the supernatants after 7 days of differentiation from either podocytes or epithelial cells under NG/HG and with/without Ladarixin treatment before and upon 24 h incubation on healthy leucocytes.

In the supernatants from podocytes, IL-8, IL-6, GM-CSF and TNF- α levels were increased, though not significantly, under HG versus NG conditions, and a slight, not significant enhancement was observed in presence of 1 μ M and 10 μ M Ladarixin either in NG or HG (Table S1). Consistent with ELISA data (Figure 3), these differences were not present in supernatants from epithelial cells. However, in these cells 10 μ M Ladarixin treatment induced a general dampening of pro-inflammatory cytokines, among which IL-1 β , IL-8, GM-CSF, MIP-1 β , RANTES, and TNF- α (Table S2).

In HG, a slight increase in IL-13, FGF-b and RANTES was observed in podocyte-conditioned media co-incubated with leucocytes. In the presence of ladarixin-treated podocytes, a significant reduction of the chemokine RANTES was detected (Table S3).

Conversely, upon incubation with leucocytes, in HG, epithelial cell media displayed a slight increase in IL-6 and RANTES. No significant effects were observed upon ladarixin treatment (Table S3).

These results suggest a differential involvement of epithelial and podocyte cells in DN pathogenesis, which leads to a differential Ladarixin effect on epithelial cells, podocytes and leucocytes contribution to disease progression (Figure 5).

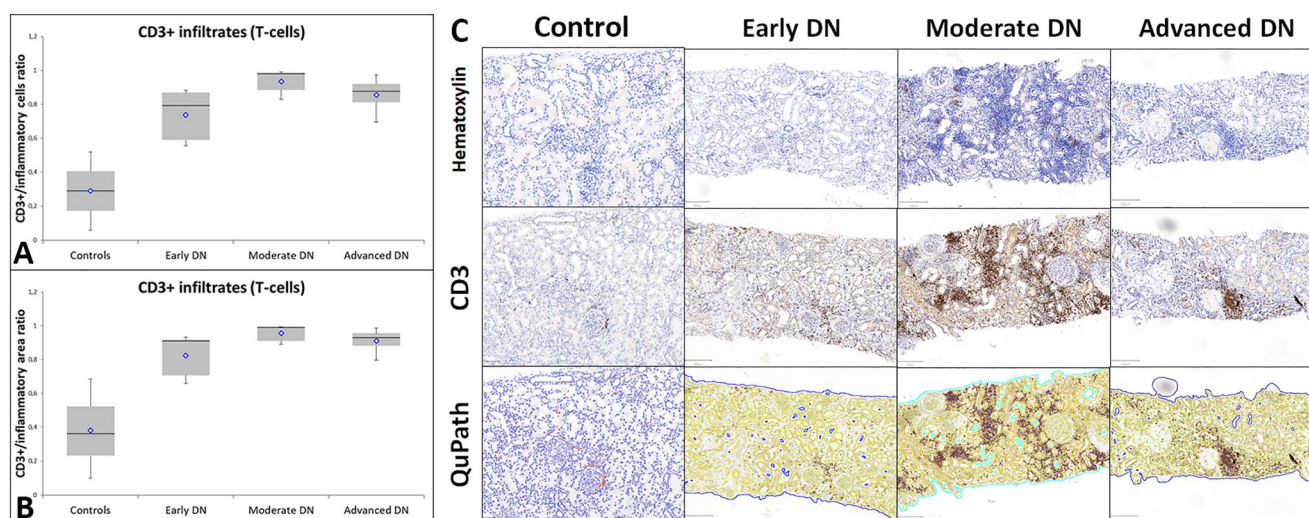


FIGURE 4 The analysis of T-lymphocyte infiltrates through a digital counting of CD3+ cells in the biopsies demonstrated a trend towards an increase in these cells from controls to advanced DN, with CD3+/inflammatory cells (A) nor CD3+/inflammatory cells area (B) ratios showing a statistically significant difference among groups (p values of *0.0002 and *0.0007, respectively), as demonstrated by the histological pictures of the cases showing the T-cell infiltrates increasing from controls to advanced DN (C).

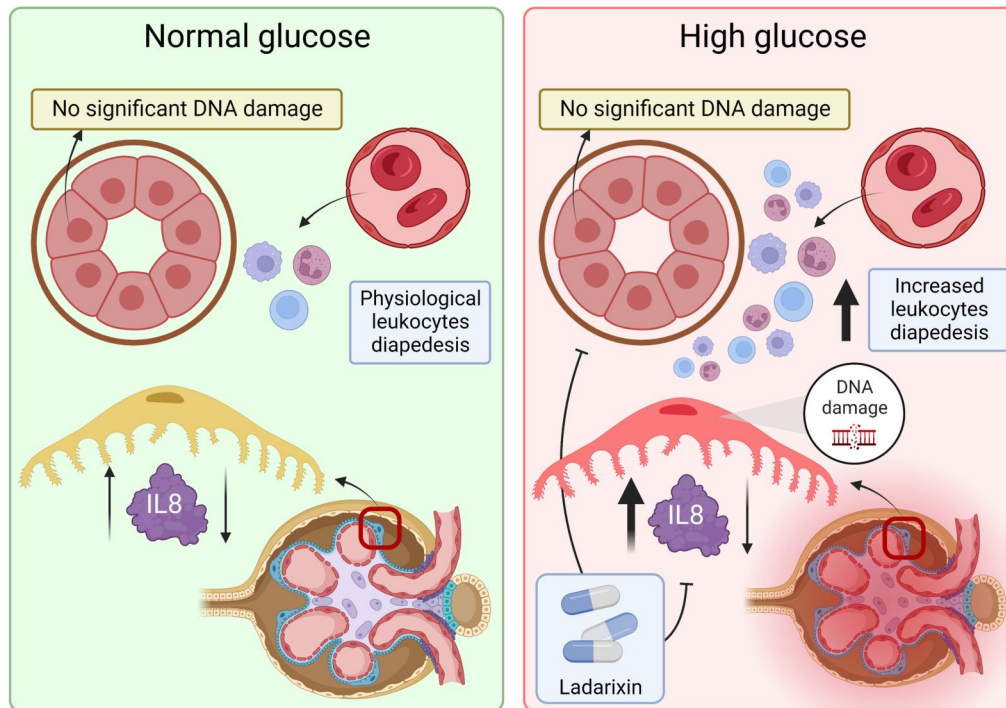


FIGURE 5 Schematic representation of the physiological and high glucose model demonstrated in the study. In physiological glucose conditions, tubular epithelial cells do not demonstrate significant DNA damage and the leucocytes are subject to physiological diapedesis with balanced production of IL-8 by podocytes. The presence of high glucose induces the over-production of IL-8 with consequent increased leucocyte diapedesis and concurrent DNA damage to the podocytes but not tubular cells. Ladarixin can act in this setting by inhibiting the IL8 loop.

4 | DISCUSSION

To date, no completely effective therapeutic approaches are available for the treatment of DN. Recently, IL-8- CXCR1/2 axis has been found to be involved in podocyte damage in DN, and its inhibition has been proposed as a potential therapeutic strategy.¹⁴ In the present study, we used an innovative model of human syngenic cultures of podocytes and tubular epithelial cells from the differentiation of human NS to shed light on the mechanisms underlying the role of IL-8- CXCR1/2 axis in DN. We demonstrated that HG can induce per se an increase in IL-8 gene expression and protein release in podocytes but not in tubular epithelial cells, and these effects were associated with DNA damage in NS-derived podocytes and, notably, also in biopsies from patients with DN at different stages. In this context, IL-8- CXCR1/2 axis inhibition by Ladarixin prevented HG-induced increase in IL-8 gene expression in podocytes and of IL-8-mediated DNA damage, thus suggesting a potential effect of the molecule in counteracting podocyte damage and loss in DN.

The first point of innovation of the present study lies in the use of a human NS model to investigate the role of the IL-8-CXCR1/2 axis. This model^{15,35} represents in fact a unique tool and a human source of primary renal cells, with emphasis on podocytes, which are normally difficult to isolate and can be cultured only upon immortalisation.³⁶ In a previous study, Loretelli et al. showed that in vitro challenge of human immortalised podocytes with HG resulted in increased IL-8 secretion and DNA damage, and that this damage is

prevented by CXCR1/2 blockade.¹⁴ Starting from these data, we demonstrated that NS cells can be used to study the IL-8-CXCR1/2 axis as they expressed CXCR1/2, while NS cell-differentiated podocytes and epithelial cells expressed CXCR2. Moreover, we showed that exposure to exogenous IL-8 under NG-induced DNA damage in podocytes but not in epithelial cells, similar to that induced by HG. However, exogenous IL-8 did not enhance DNA injury that was induced by HG, suggesting that hyperglycemia is sufficient to reproduce in vitro the effects that at least in part may be mediated in vivo by podocyte-autocrine IL-8 production.

As a result of the noxious effects of HG and IL-8 on podocytes, we observed increased DNA damage in podocytes from NS that was confirmed in human biopsies from early to moderate stages of DN. The relationship between DNA damage and loss of podocytes is already well established.^{37,38} In particular, HG conditions were proposed to induce genomic and mitochondrial DNA damage in podocytes^{39,40} suggesting that protection from DNA damage and promotion of DNA repair in podocytes is an important treatment strategy for DN. Interestingly, the analysis on human biopsies showed that, with the progression of DKD, the damage can involve precursors/progenitor cells of the podocytes. In particular, we detected γ -H2AX positivity in flat parietal epithelial cells entrapped in the global sclerosis of end-stage glomeruli, and this may be a consequence of a progressive recruitment of reservoir cells after the loss of podocytes that hesitate in the extension of DNA damage even to those precursor cells.⁴¹ This pattern correlates with increasing T-cell infiltration during disease

progression, although no direct correlation among the increase in IL-8 and the progressive lymphocyte interstitial infiltration has been demonstrated in the present study. For this reason and for the fact that in these patients a mixed aetiology of the renal damage cannot be excluded, further investigations on this aspect are required.

To assess the effect of CXCR2 blockade on podocytes independently of the immune component, we evaluated cell survival and differentiation in either podocyte or epithelial cell cultures after treatment with a CXCR1/2 antagonist molecule, Ladarixin, which is currently being tested in a phase 3 clinical trial for the treatment of new-onset type 1 diabetes (T1D) ([ClinicalTrials.gov Identifier: NCT04628481](https://clinicaltrials.gov/ct2/show/study/NCT04628481)). Notably, being an allosteric non-competitive inhibitor, Ladarixin is able to bind CXCR1/2 in a different site compared to IL-8, thus allowing the maintenance of the ligand-receptor homeostasis. Ladarixin treatment throughout the differentiation under HG challenge prevented the increase in IL-8 gene expression in podocytes, with a significant reduction of IL8-mediated DNA damage, while, coherently with the mechanism of action of the drug, it did not significantly affect IL-8 secretion. Consistently, exogenous IL-8 did not induce further DNA damage in podocytes compared with HG alone. To investigate more deeply into the mechanism of action of CXCR1/2 antagonists in the mutual IL-8-mediated modulation of immune/renal cells axis, we performed a cytokine patterning of the supernatants from podocytes under all treatment conditions and we detected a specific increase in IL-8 under HG compared to NG, on which, consistent with our data from ELISA, Ladarixin treatment showed no effect.

After incubation of the same supernatants on leucocytes, a slight enhancement of IL-8 secretion was detectable in the supernatants from HG cultured podocytes, likely suggesting a mild podocyte-mediated attraction rather than activation of leucocytes. According to this hypothesis, only a slight dampening of RANTES^{42,43} was observed in supernatants from podocytes treated with Ladarixin and incubated on leucocytes. Conversely, in epithelial cell media, upon incubation with leucocytes, we observed a slight increase in IL-6 and RANTES levels, with no significant effects on Ladarixin treatment.

These results suggest that CXCR2 is activated both in epithelial and podocyte cells, with a differential involvement in DN pathogenesis. In podocytes, the activation of CXCR2 under NG is likely involved in self-maintenance and becomes impaired under stress conditions through endogenous IL-8-induced DNA damage and the attraction of immune cells. In epithelial cells, CXCR2 activation under NG is likely involved in the maintenance of resident immune surveillance and increases under more general disease-induced pro-inflammatory conditions.

Interestingly, previous evidence showed that CXCR1/2 blockade reduced albuminuria and decreased mesangial expansion and podocyte apoptosis in diabetic db/db mice.¹⁴ Further Pawlick et al.⁴⁴ showed reduced kidney T-cell infiltration and neutrophil activation in a murine islet allotransplant model after combined treatment with CXCR1/2 antagonist and CTLA4-Ig.

Though beyond the aim of the present study, it is important to remark that in our experimental setting, the role played in DN by

renal glomerular endothelial cells was overlooked.⁴⁵ Future studies will be needed to assess the multifaceted cross-talk among podocytes, tubular epithelial, endothelial and immune cells.

In summary, using a multipotent nephrogenic human cell model, we assessed the role of IL-8/CXCR2 pathway in DN, and our results suggest that CXCR1-2 antagonism by Ladarixin can be a potential therapeutic strategy to exert an anti-inflammatory effect on epithelial cell and leucocyte activation, and a more specific protective effect on podocyte survival.

AUTHOR CONTRIBUTIONS

Chiara Grasselli and Silvia Bombelli: Experiment execution (nephrosphere culture and characterisation and treatment), data analysis and manuscript writing. **Vittoria D'Esposito, Michele Francesco Di Tolla, Francesca Rocchio, Martina Sara Miscione, Pietro Formisano:** Experiment execution (lymphocyte cultures), data analysis and manuscript writing. **Vincenzo L'Imperio and Fabio Pagni:** Experiment execution (IH of human tissues) and data analysis. **Rubina Novelli and Pier Adelchi Ruffini:** Manuscript revision and scientific support. **Andrea Aramini, Marcello Allegretti and Roberto Perego:** Scientific support and management of collaboration and funding and final approval. **Lidia De Filippis:** Experimental design, experiment execution, data analysis, manuscript writing and management of collaboration.

ACKNOWLEDGEMENTS

The project was funded by Dompè as part of the activities planned in the co-financed project 'Ladarixin as new Juvenile Diabetes Inhibitory Agent (LJDIA)' presented by Dompè under the call 'Fondo crescita sostenibile-Proposal n. 1410-bando MISE DM 02/0872019 and consecutive DD 02/10/2019'. In particular, most of the experiments described in this study were planned according to a Research Agreement between Dompè Pharmaceuticals and Dept Medicine and Surgery, in the lab directed by Roberto Perego.

CONFLICT OF INTEREST STATEMENT

Francesca Rocchio, Martina Sara Miscione, Rubina Novelli, Pier Adelchi Ruffini, Andrea Aramini, Marcello Allegretti, and Lidia De Filippis are employees of Dompè Farmaceutici S.p.A., Italy. The other authors declare no conflicts of interest.

ETHICS STATEMENT

All procedures reported in the manuscript were performed after written patient consent and were approved by the Local Ethical Committee.

DATA AVAILABILITY STATEMENT

The data that support the findings of this study are available from the corresponding author upon reasonable request.

ORCID

Michele Francesco Di Tolla  <https://orcid.org/0000-0002-1376-3782>

Francesca Rocchio  <https://orcid.org/0000-0002-2145-2642>

Pier Adelchi Ruffini  <https://orcid.org/0000-0001-9492-9627>

Roberto Perego  <https://orcid.org/0000-0003-3053-3476>

PEER REVIEW

The peer review history for this article is available at <https://www.webofscience.com/api/gateway/wos/peer-review/10.1002/dmrr.3694>.

REFERENCES

- Saran R, Robinson B, Abbott KC, et al. US renal data system 2017 annual data report: epidemiology of kidney disease in the United States. *Am J Kidney Dis*. 2018;71(3 Suppl 1):A7. <https://doi.org/10.1053/j.ajkd.2018.01.002>
- Niewczas MA, Pavkov ME, Skupien J, et al. A signature of circulating inflammatory proteins and development of end-stage renal disease in diabetes. *Nat Med*. 2019;25(5):805-813. <https://doi.org/10.1038/s41591-019-04155>
- Bussolati B, Bruno S, Grange C, et al. Isolation of renal progenitor cells from adult human kidney. *Am J Pathol*. 2005;166(2):545-555. [https://doi.org/10.1016/S0002-9440\(10\)62276-6](https://doi.org/10.1016/S0002-9440(10)62276-6)
- Fiorina P, Vergani A, Bassi R, et al. Role of podocyte B7-1 in diabetic nephropathy. *J Am Soc Nephrol*. 2014;25(7):1415-1429. <https://doi.org/10.1681/ASN.2013050518>
- Baragetti I, El Essawy B, Fiorina P. Targeting immunity in end-stage renal disease. *Am J Nephrol*. 2017;45(4):310-319. <https://doi.org/10.1159/000458768>
- Bassi R, Fornoni A, Doria A, Fiorina P. CTLA4-Ig in B7-1-positive diabetic and non-diabetic kidney disease. *Diabetologia*. 2016;59(1):21-29. <https://doi.org/10.1007/s00125-015-3766-6>
- Solini A, Usuelli V, Fiorina P. The dark side of extracellular ATP in kidney diseases. *J Am Soc Nephrol*. 2015;26(5):1007-1016. <https://doi.org/10.1681/ASN.2014070721>
- Wolkow PP, Niewczas MA, Perkins B, et al. Association of urinary inflammatory markers and renal decline in microalbuminuric type 1 diabetics. *J Am Soc Nephrol*. 2008;19(4):789-797. <https://doi.org/10.1681/ASN.2007050556>
- Tashiro K, Koyanagi I, Saitoh A, et al. Urinary levels of monocyte chemoattractant protein-1 (MCP-1) and interleukin-8 (IL-8), and renal injuries in patients with type 2 diabetic nephropathy. *J Clin Lab Anal*. 2002;16(1):1-4. <https://doi.org/10.1002/jcla.2057>
- Scurt FG, Menne J, Brandt S, et al. Monocyte chemoattractant protein-1 predicts the development of diabetic nephropathy. *Diabetes Metab Res Rev*. 2022;38(2):e3497. <https://doi.org/10.1002/dmrr.3497>
- Huber TB, Reinhardt HC, Exner M, et al. Expression of functional CCR and CXCR chemokine receptors in podocytes. *J Immunol*. 2002;168(12):6244-6252. <https://doi.org/10.4049/jimmunol.168.12.6244>
- Mikacenic C, Hahn WO, Price BL, et al. Biomarkers of endothelial activation are associated with poor outcome in critical illness. *PLoS One*. 2015;10(10):e0141251. <https://doi.org/10.1371/journal.pone.0141251>
- Barchetta I, Cimini FA, Capoccia D, et al. WISP1 is a marker of systemic and adipose tissue inflammation in dysmetabolic subjects with or without type 2 diabetes. *J Endocr Soc*. 2017;1(6):660-670. <https://doi.org/10.1210/je.2017-00108>
- Loretelli C, Rocchio F, D'Addio F, et al. The IL-8-CXCR1/2 axis contributes to diabetic kidney disease. *Metabolism*. 2021;121:154804. <https://doi.org/10.1016/j.metabol.2021.154804>
- Bombelli S, Zipeto MA, Torsello B, et al. PKHhigh cells within clonal human nephrospheres provide a purified adult renal stem cell population. *Stem Cell Res*. 2013;11(3):1163-1177. <https://doi.org/10.1016/j.scr.2013.08.004>
- Dontu G, Abdallah WM, Foley JM, et al. In vitro propagation and transcriptional profiling of human mammary stem/progenitor cells. *Genes Dev*. 2003;17(10):1253-1270. <https://doi.org/10.1101/gad.1061803>
- Steinberg OH, Omer D, Gnatek Y, et al. Ex vivo expanded 3D human kidney spheres engraft long term and repair chronic renal injury in mice. *Cell Rep*. 2019;30(3):852-869. <https://doi.org/10.1016/j.celrep.2019.12.047>
- Bianchi C, Bombelli S, Raimondo F, et al. Primary cell cultures from human renal cortex and renal-cell carcinoma evidence a differential expression of two spliced isoforms of annexin A3. *Am J Pathol*. 2010;176(4):1660-1670. <https://doi.org/10.2353/ajpath.2010.090402>
- Cifola I, Bianchi C, Mangano E, et al. Renal cell carcinoma primary cultures maintain genomic and phenotypic profile of parental tumor tissues. *BMC Cancer*. 2011;11(1):244. <https://doi.org/10.1186/1471-2407-11-244>
- D'Esposito V, Di Tolla MF, Lecce M, et al. Lifestyle and dietary habits affect plasma levels of specific cytokines in healthy subjects. *Front Nutr*. 2022;9:913176. <https://doi.org/10.3389/fnut.2022.913176>
- Cohen Tervaert TW, Mooyaart AL, Amann K, et al. Pathologic classification of diabetic nephropathy. *J Am Soc Nephrol*. 2010;21(4):556-563. <https://doi.org/10.1681/ASN.2010010010>
- L'Imperio V, Pieruzzi F, Sinico RA, et al. Routine immunohistochemical staining in membranous nephropathy: in situ detection of phospholipase A2 receptor and thrombospondin type 1 containing 7A domain. *J Nephrol*. 2018;31(4):543-550. <https://doi.org/10.1007/s40620-018-0489-z>
- L'Imperio V, Pieruzzi F, Sinico RA, et al. Combined plasmatic and tissue approach to membranous nephropathy-proposal of a diagnostic algorithm including immunogold labelling: changing the paradigm of a serum-based approach. *Appl Immunohistochem Mol Morphol*. 2020;28(5):376-383. <https://doi.org/10.1097/PAI.0000000000000753>
- L'Imperio V, Casati G, Cazzaniga G, et al. Improvements in digital pathology equipment for renal biopsies: updating the standard model. *J Nephrol*. 2023. <https://doi.org/10.1007/s40620-023-01568-1>
- QuPath: Open source software for digital pathology image analysis. Bankhead P, Loughrey MB, Fernández JA, et al. *Scientific Reports*. 2017;7:16878. <https://doi.org/10.1038/s41598-017-17204-5>
- Kanauchi M, Nishioka H, Hashimoto T. Oxidative DNA damage and tubulointerstitial injury in diabetic nephropathy. *Nephron*. 2002;91(2):327-329. <https://doi.org/10.1159/000058412>
- Xu GW, Yao QH, Weng QF, Su B, Zhang X, Xiong J. Study of urinary 8-hydroxydeoxyguanosine as a biomarker of oxidative DNA damage in diabetic nephropathy patients. *J Pharm Biomed Anal*. 2004;36(1):101-104. <https://doi.org/10.1016/j.jpba.2004.04.016>
- Altındağ F, Özdek U. Synergistic effects of sinapic acid and ellagic acid ameliorate streptozotocin-induced diabetic nephropathy by inhibiting apoptosis, DNA damage, and structural deterioration in rats. *Hum Exp Toxicol*. 2021;40(12_Suppl 1):S290-S299. <https://doi.org/10.1177/09603271211040825>
- Moriconi A, Cesta MC, Cervellera MN, et al. Design of noncompetitive interleukin-8 inhibitors acting on CXCR1 and CXCR2. *J Med Chem*. 2007;50(17):3984-4002. <https://doi.org/10.1021/jm061469t>
- Bertini R, Barcelos LS, Beccari AR, et al. Receptor binding mode and pharmacological characterization of a potent and selective dual CXCR1/CXCR2 non-competitive allosteric inhibitor. *Br J Pharmacol*. 2012;165(2):436-454. <https://doi.org/10.1111/j.14765381.2011.01566.x>
- Garau A, Bertini R, Mosca M, et al. Development of a systemically-active dual CXCR1/CXCR2 allosteric inhibitor and its efficacy in a model of transient cerebral ischemia in the rat. *Eur Cytokine Netw*. 2006;17:35-41.

32. Citro A, Valle A, Cantarelli E, et al. CXCR1/2 inhibition blocks and reverses type 1 diabetes in mice. *Diabetes*. 2015;64(4):1329-1340. <https://doi.org/10.2337/db14-0443>
33. ZhouLiuHu WYQ, Zhou J, Lin H. The landscape of immune cell infiltration in the glomerulus of diabetic nephropathy: evidence based on bioinformatics. *BMC Nephrol*. 2022;23(1):303. <https://doi.org/10.1186/s12882-022-02906-4>
34. Ruster C, Wolf G. The role of chemokines and chemokine receptors in diabetic nephropathy. *Front Biosci*. 2008;13:944-955. <https://doi.org/10.2741/2734>
35. Bombelli S, Meregalli C, Grasselli C, et al. PKHhigh/CD133+/CD24– renal stem-like cells isolated from human nephrospheres exhibit in vitro multipotency. *Cells*. 2020;9(8):1805. <https://doi.org/10.3390/cells9081805>
36. Agarwal S, Sudhini YR, Reiser J, Altintas MM. From infancy to fancy: a glimpse into the evolutionary journey of podocytes in culture. *Kidney360*. 2021;2(2):385-397. <https://doi.org/10.34067/KID.0006492020>
37. Zhu Y.-T, Wan C, Lin J.-H, Hammes HP, Zhang C. Mitochondrial oxidative stress and cell death in podocytopathies. *Biomolecules*. 2022;12(3):403. <https://doi.org/10.3390/biom12030403>
38. Marshall CB, Pippin JW, Krofft RD, Shankland S. Puromycin aminonucleoside induces oxidant-dependent DNA damage in podocytes in vitro and in vivo. *Kidney Int*. 2006;70(11):1962-1973. <https://doi.org/10.1038/sj.ki.5001965>
39. Hishikawa A, Hayashi K, Abe T, et al. Decreased KAT5 expression impairs DNA repair and induces altered DNA methylation in kidney podocytes. *Cell Rep*. 2019;26(5):1318-1332.e4. <https://doi.org/10.1016/j.celrep.2019.01.005>
40. Wu GJ, Zhao HB, Zhang XW, et al. Death-associated protein kinase 1 correlates with podocyte apoptosis and renal damage and can be mediated by miR-361. *Histol Histopathol*. 2021;36(11):1155-1167. <https://doi.org/10.14670/HH-18-358>
41. Shankland SJ, Anders H, Romagnani P. Glomerular parietal epithelial cells in kidney physiology, pathology, and repair. *Curr Opin Nephrol Hypertens*. 2013;22(3):302-309. <https://doi.org/10.1097/MNH.0b013e32835fed4>
42. Navarro-González JF, Mora-Fernández C, Muros de Fuentes M, García-Pérez J. Inflammatory molecules and pathways in the pathogenesis of diabetic nephropathy. *Nat Rev Nephrol*. 2011;7(6):327-340. <https://doi.org/10.1038/nrneph.2011.51>
43. Araújo LS, Torquato BGS, Aparecida da Silva C, et al. Renal expression of cytokines and chemokines in diabetic nephropathy. *BMC Nephrol*. 2020;21(1):308. <https://doi.org/10.1186/s12882-020-01960-0>
44. Pawlick RL, Wink J, Pepper AL, et al. Reparixin, a CXCR1/2 inhibitor in islet allotransplantation. *Islets*. 2016;8(5):115-124. <https://doi.org/10.1080/19382014.2016.1199303>
45. Liang X, Fengmin S. Sitagliptin protects renal glomerular endothelial cells against high glucose-induced dysfunction and injury. *Bioengineered*. 2022;13(1):655-666. <https://doi.org/10.1080/21655979.2021.2012550>

SUPPORTING INFORMATION

Additional supporting information can be found online in the Supporting Information section at the end of this article.

How to cite this article: Grasselli C, Bombelli S, D'Esposito V, et al. The therapeutic potential of an allosteric non-competitive CXCR1/2 antagonist for diabetic nephropathy. *Diabetes Metab Res Rev*. 2023;39(7):e3694. <https://doi.org/10.1002/dmrr.3694>